Stability Analysis of a Matrix Converter Drive: Effects of Input Filter Type and the Voltage Fed to the Modulation Algorithm

M. H. Abardeh*[(C.A.)] and R. Ghazi*

Abstract: The matrix converter instability can cause a substantial distortion in the input currents and voltages which leads to the malfunction of the converter. This paper deals with the effects of input filter type, grid inductance, voltage fed to the modulation algorithm and the synchronous rotating digital filter time constant on the stability and performance of the matrix converter. The studies are carried out using eigenvalues of the linearized system and simulations. Two most common schemes for the input filter (LC and RLC) are analyzed. It is shown that by a proper choice of voltage input to the modulation algorithm, structure of the input filter and its parameters, the need for the digital filter for ensuring the stability can be resolved. Moreover, a detailed model of the system considering the switching effects is simulated and the results are used to validate the analytical outcomes. The agreement between simulation and analytical results implies that the system performance is not deteriorated by neglecting the nonlinear switching behavior of the converter. Hence, the eigenvalue analysis of the linearized system can be a proper indicator of the system stability.

Keywords: Digital Filter, Eigenvalue Analysis, Input Filter, Matrix Converter, Small Signal Model, Stability.

1 Introduction

The Matrix Converters (MC) have received considerable attention in recent years, as they can be an alternative to back-to-back converters. The main reasons are their ability to provide sinusoidal input and output waveforms, controllable input power factor and bidirectional power flow in the absence of DC bus [1, 2]. This eliminates the electrolytic capacitor and provides the possibility of a compact design [3]. The MC main application fields are: AC motor drives, wind energy conversion systems, aerospace and military applications, elevators with energy recovery systems, electric and hybrid vehicles, etc. [4, 5].

As the matrix converter connects two systems with different frequencies without any intermediate energy storage unit, the input distortions are easily transferred to the output side. To overcome this problem, the fast feedforward compensation is used in which the modulation algorithm variables are calculated based on

the instantaneous input voltages. The input LC or RLC filter in conjunction with the feedforward compensation may cause unstable behavior [6-8].

Several methods have been proposed to account for the causes and criterions of the matrix converter unstable operation [6-16]. Small signal approximation and state matrix eigenvalues are used in [6] to model and analyze the stability problem. Two types of LC and RLC input filters are studied, and it is shown that a proper choice of the filter resistor can improve stability. The factors that influence the stability of the MC fed to a passive RL load or an induction motor are analyzed by calculating eigenvalues in [7] and concluded that the independent filtering of input voltage amplitude and phase data will improve the stability. The effects of various input filter structure C, LC and LCR under the Venturini modulation algorithm are considered in [9]. Authors of [8] have indicated that the cause of unstable operation is the harmonic interactions of the MC input voltage and current. Moreover, the digital controller delay and power loss can change the stability characteristics of the MC drive [15]. There is an upper bound for the MC output power which limits the drive performance, but it is shown that the stable operation region can be extended when the voltage fed to the

modulation algorithm is filtered by a low pass synchronous rotating filter. The effect of the time constant of the voltage filter is studied in [10]. Eigenvalue analysis shows the larger time constants will improve the stability while lowers the system ability to compensate for the input voltage distortions. A large signal model for stability analysis is introduced in [11] and the power limit for stable operation is found as a function of different system parameters such as input filter, digital implementation time delay, time constant, and order of the input digital filter.

By introducing a switching model, the effects of high frequency switching on the MC stability is studied in [12]. It is shown that using the average model leads to underestimation of the instability threshold. However, it is notified in [12] that when double-sided modulation is used, the results obtained from the average model are valid. Matrix converter experiences Hopf bifurcation instability as the input/output voltage ratio of the MC becomes greater than a threshold [13]. A weakly nonlinear analysis is developed and it is concluded that even when the MC operates below the linear stability limit, large-amplitudes oscillations may occur. Moreover, in [13] an interesting discussion on the switching effect in the stability analysis is presented. Using the nonlinear dynamic theory, the unstable oscillation of the MC is studied in [16] and the chaotic characteristic such as extreme sensitivity to initial values within the system is analyzed.

As it was mentioned when the input voltage to the modulation algorithm is filtered by a synchronous rotating filter before being fed to the algorithm, the stability will be improved. However, this will make the system more complicated as filtering is performed in the dq reference frame which necessitates the *abc* to *dq* and inverse transformations. Moreover, the filtering action of such a filter reduces the speed of system response to the input voltage distortions because the modulation algorithm is now not fed by actual instantaneous voltage. To improve the operating performance, in this paper the effects of the input filter type (LC and RLC), the digital filter time constant and the voltage fed to the modulation algorithm on the stability of a matrix converter connected to an RL load is studied. The linearized state space equations of the system are presented, and the obtained eigenvalues are used to identify the stable operating region. To eliminate the need for the digital rotating synchronous filter and its attendant disadvantages a suitable point of modulation voltage measurement along with input filter type and its parameters are suggested. Simulation of the detailed system by considering the switching behavior of the power switches of the matrix converter controlled by SVM algorithm is used to validate the results of the eigenvalue analysis.

This paper is organized as follows. The model of the benchmark system is presented in Section. 2. The stability analysis based on the system eigenvalues is carried out in Section. 3. The effect of the input filter on the power loss and voltage drop of the input filter is presented in Section. 4. Simulation results are demonstrated in Section. 5. Finally Section. 6 concludes the paper.

2 Matrix Converter Model

The basic scheme of a matrix converter is shown in Fig. 1. The bidirectional switches have common emitter or common collector configuration. According to [17], the relation between the space vectors of input and output voltages and currents can be represented by

$$\bar{v}_o = \frac{3}{2}\bar{v}_i.\bar{m}_i^* + \frac{3}{2}\bar{v}_i^*.\bar{m}_d \qquad (1)$$

$$\bar{i}_i = \frac{3}{2}\bar{i}_o.\bar{m}_i + \frac{3}{2}\bar{i}_o^*.\bar{m}_d \qquad (2)$$

The modulation indices $\bar{m}_d$ and $\bar{m}_i$ are:

$$\bar{m}_d = \frac{\bar{v}_{o,ref}}{3\bar{v}_{im}^*} \qquad (3)$$

$$\bar{m}_i = \frac{\bar{v}_{o,ref}^*}{3\bar{v}_{im}^*} \qquad (4)$$

where $\bar{v}_{o,ref}$ is the output voltage reference and $\bar{v}_{im}$ is the voltage input into the modulation algorithm. In these equations the switching frequency is supposed to be much higher than the input and output frequency. Moreover, the on and off-times of switches are neglected as are very small regarding the switching frequency.

The benchmark system is shown in Fig. 2. With respect to this configuration $\bar{v}_{im}$ can be measured at different points.
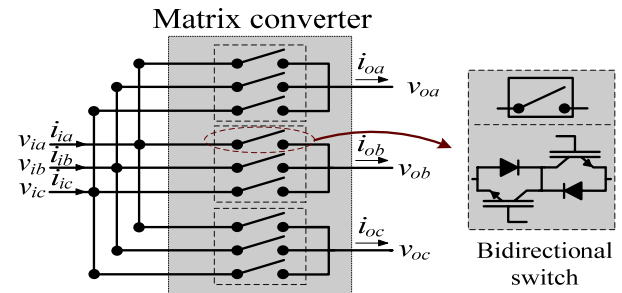

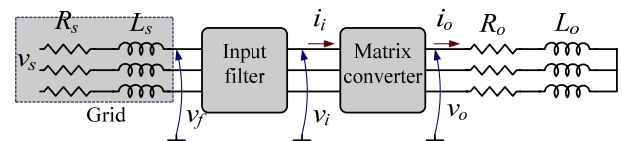**Fig. 1** Basic scheme of matrix converter.

Fig. 2 Benchmark system of matrix converter drive.

So the following four cases are suggested and the stability analysis is evaluated:

1) The voltage input to the modulation algorithm is measured at MC input ($\bar{v}_{im} = \bar{v}_i$), and the LC input filter is used.

2) The voltage input to the modulation algorithm is measured at input filter ($\bar{v}_{im} = \bar{v}_f$), and the LC input filter is used.

3) The voltage input to the modulation algorithm is measured at MC input ($\bar{v}_{im} = \bar{v}_i$), and the RLC input filter is used.

4) The voltage input to the modulation algorithm is measured at input filter ($\bar{v}_{im} = \bar{v}_f$), and the RLC input filter is used.

The small signal model of the system is developed for each case, and the stability of the system is analyzed using the eigenvalues.

2.1 Case 1: LC Input Filter and $\bar{v}_{im} = \bar{v}_i$

The LC filter type is shown in Fig. 3. It is supposed that the modulation input voltage is measured at matrix converter input. At the input side, we have:

$$\frac{d}{dt}\bar{i}_s = -(\frac{R_s}{L_t} + j\omega_i)\bar{i}_s - \frac{1}{L_t}(\bar{v}_i - \bar{v}_s) \tag{5}$$

where $L_t = L_S + L_f$ and ω_i is the source angular frequency. The input filter capacitor voltage is:

$$\frac{d}{dt}\bar{v}_i = \frac{1}{C_f}\bar{i}_s - j\omega_i\bar{v}_i - \frac{1}{C_f}\bar{i}_i \tag{6}$$

The series resistance of the input filter capacitor is neglected. To improve the stability, a first order low pass synchronous rotating filter is utilized to filter the input voltage before applying it to the modulation algorithm [10]. Therefore, the filtered voltage is

$$\frac{d}{dt}\bar{v}_{if} = \frac{1}{\tau}\bar{v}_{im} - \frac{1}{\tau}\bar{v}_{if} \tag{7}$$

where τ is the filter time constant and $\bar{v}_{im}$ is the voltage input to the modulation algorithm. The MC output current space vector is:

$$\frac{d}{dt}\bar{i}_o = -(\frac{R_o}{L_o} + j\omega_o)\bar{i}_o + \frac{1}{L_o}\bar{v}_o \tag{8}$$
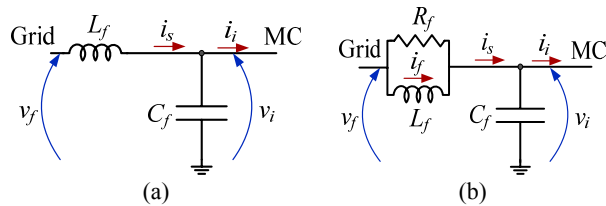

Fig. 3 Input filter types (a) LC and (b) RLC.

where ω_o is the MC output side angular frequency.

The equations describing the matrix converter steady state operation are:

$$\bar{V}_{if} = \bar{V}_{im} \tag{9}$$

$$M_d = \frac{q}{3} \tag{10}$$

$$M_i = \frac{q}{3} \tag{11}$$

$$\bar{V}_o = q\bar{V}_{im} \tag{12}$$

where q represents the MC input to output voltage ratio. The output and input side steady state currents are:

$$\bar{I}_o = \frac{q\bar{V}_i}{Z_o} \tag{13}$$

$$\bar{I}_i = \frac{R_o}{Z_o^2}q^2\bar{V}_i \tag{14}$$

and the source current and voltage are:

$$\bar{I}_s = (j\omega_i C_f + \frac{R_o}{Z_o^2}q^2)\bar{V}_i \tag{15}$$

$$\bar{V}_s = (1 + j\omega_i C_f Z_i + \frac{R_o Z_i}{Z_o^2}q^2)\bar{V}_i \tag{16}$$

where the input and output side impedances are defined by:

$$Z_i = R_s + j\omega_i L_t \tag{17}$$

$$Z_o = R_o + j\omega_o L_o \tag{18}$$

The state space representation of the system is as follows

$$\frac{d}{dt}\bar{X} = A\bar{X} + B\bar{u} \tag{19}$$

Equations (1)-(8) are linearized around steady state operating point calculated by Eqs. (9)-(17). Considering the following vector of the state variables

$$\bar{X} = [\Delta i_{sd}, \Delta i_{sq}, \Delta v_{id}, \Delta v_{iq}, \Delta i_{od}, \Delta i_{oq}, ...$$

$$\Delta v_{ifd}, \Delta v_{ifq}]^T \tag{20}$$

leads to

$$\mathbf{A} = \mathbf{A}_1 = \begin{bmatrix} \mathbf{A}_{11} & \mathbf{A}_{12} \end{bmatrix} \tag{21}$$

where $\mathbf{A}_{11}$ and $\mathbf{A}_{12}$ are presented in the appendix.

The matrix **B** is not represented here because it has no effect on the stability.

2.2 Case 2: LC input filter and $\bar{v}_{im} = \bar{v}_f$

It is supposed that the modulation input voltage is measured at input filter ($\bar{v}_{im} = \bar{v}_f$) where $\bar{v}_f$ can be calculated from following:

$$\bar{v}_f = L_f \frac{d}{dt}\bar{i}_s + j\omega_i\bar{i}_s + \bar{v}_i \tag{22}$$

Therefore, after some manipulation we have:

$$\mathbf{A} = \mathbf{A}_2 = \begin{bmatrix} \mathbf{A}_{21} & \mathbf{A}_{22} \end{bmatrix} \tag{23}$$

where $\mathbf{A}_{21}$ and $\mathbf{A}_{22}$ are presented in the appendix.

2.3 Case 3: RLC input filter and $\overline{v}_{im} = \overline{v}_i$

The schematic of the proposed RLC filter is shown in Fig. 3(b). The source voltage is

$$\overline{v}_s = R_s \overline{i}_s + L_s \left(\frac{d}{dt} + j\omega_i\right)\overline{i}_s + \overline{v}_f \qquad (24)$$

The standard state space representation of Eq. (24) is:

$$\frac{d}{dt}\overline{i}_s = \frac{1}{L_s}\overline{v}_s - \frac{1}{L_s}\overline{v}_f - \frac{R_s}{L_s}\overline{i}_s - j\omega_i\overline{i}_s \qquad (25)$$

The input filter inductor current is a state variable defined by:

$$\frac{d}{dt}\overline{i}_f = \frac{1}{L_f}\overline{v}_f - \frac{1}{L_f}\overline{v}_i - j\omega_i\overline{i}_f \qquad (26)$$

If the source voltage $\overline{v}_s$ is ideal and without distortion. The new state variables vector is:

$$\overline{X} = [\Delta i_{sd}, \Delta i_{sq}, \Delta i_{fd}, \Delta i_{fq}, \Delta v_{id}, \Delta v_{iq},$$
$$\Delta i_{od}, \Delta i_{oq}, \Delta v_{ifd}, \Delta v_{ifq}]^T \qquad (27)$$

and the matrix **A** is

$$\mathbf{A} = \mathbf{A}_3 = \begin{bmatrix} \mathbf{A}_{31} & \mathbf{A}_{32} \end{bmatrix} \qquad (28)$$

where $\mathbf{A}_{31}$ and $\mathbf{A}_{32}$ are presented in the appendix.

2.4 Case 4: RLC input filter and $\overline{v}_{im} = \overline{v}_f$

In this case, the voltage measurement point is at the input filter that is:

$$\overline{v}_{im} = \overline{v}_f \qquad (29)$$

The linearized filter input voltage is:

$$\Delta\overline{v}_f = R_s\Delta\overline{i}_s - R_f\Delta\overline{i}_f + \Delta\overline{v}_i \qquad (30)$$

Therefore, we have:

$$\Delta\overline{v}_{if} = \frac{R_f}{\tau}\Delta\overline{i}_s - \frac{R_f}{\tau}\Delta\overline{i}_f + \frac{R_f}{\tau}\Delta\overline{v}_i - \frac{1}{\tau}\Delta\overline{v}_{if} \qquad (31)$$

The matrix **A** becomes:

$$\mathbf{A} = \mathbf{A}_4 = \begin{bmatrix} \mathbf{A}_{41} & \mathbf{A}_{42} \end{bmatrix} \qquad (32)$$

where $\mathbf{A}_{11}$ and $\mathbf{A}_{12}$ are presented in the appendix.

3 Stability Analysis

The benchmark system parameters are shown in Table 1. The stable operating region when the input filter is an LC circuit is depicted in Fig. 4. If the filter input voltage is used as the input to the modulation algorithm ($\overline{v}_{im} = \overline{v}_i$), the digital filter time constant (τ) should be at least 0.4 ms to guarantee the stability. Greater filter time constants reduce the speed of system response input side distortions. If the voltage at the filter input is fed to the modulation algorithm ($\overline{v}_{im} = \overline{v}_f$), the system becomes more stable. The digital filter time constant to ensure the stability over the entire operational region ($0.0 < q < 0.87$) is about 0.23 msec.
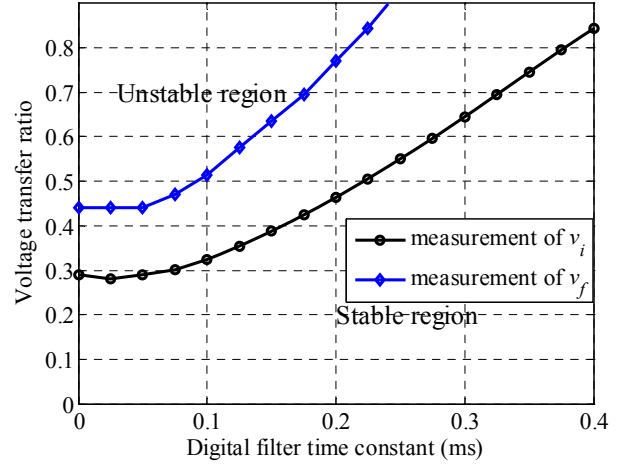

Fig. 4 Effect of voltage measurement point and digital filter time constant (RL filter case) on stability.

Table 1 Benchmark system parameters.

Parameter	Value
Source voltage	380 V (rms)
Input side frequency	50 Hz
Grid resistor	0.25 Ω
Grid inductor	0.4 mH
Filter inductor	0.6 mH
Filter capacitor	10.0 µF
Load inductor	20 mH
Load resistor	10 Ω
Output side frequency	25 Hz
Switching frequency	4.0 KHz

The effects of the network inductance, the voltage measurement point and the digital filter time constant for the LC filter case is shown in Fig. 5. It can be seen that the stable voltage ratio limit decreases as the network inductance increases regardless of the voltage measurement point. However, for the case of strong network with small inductive properties and without digital filter ($\tau = 0$), measuring v_f will obviously increase the voltage ratio limit from 0.3 to 0.9. The difference between two measurement strategies becomes smaller when a slow synchronous rotating digital filter having a large time constant ($\tau = 0.4$ msec.) is employed. The input filter voltage measurement strategy establishes stable operation in ranges ($0 < q < 0.87$) for network inductance as large as 1.0 mH. However, the MC input voltage measurement strategy leads to instability when the network inductance is greater than 0.89 mH. Finally, it can be concluded that using v_f in the modulation algorithm improves the stability of the MC drive for all network conditions.

For RLC filter case the effect of the filter resistance, the digital filter time constant and the voltage measurement point on the stability of the system is shown in Fig. 6.
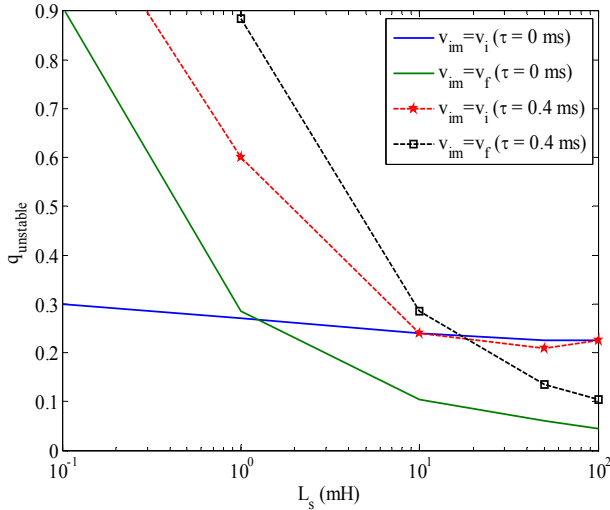
Fig. 5 Effect of network inductance, voltage measurement point and digital filter time constant (RL filter case) on stability.
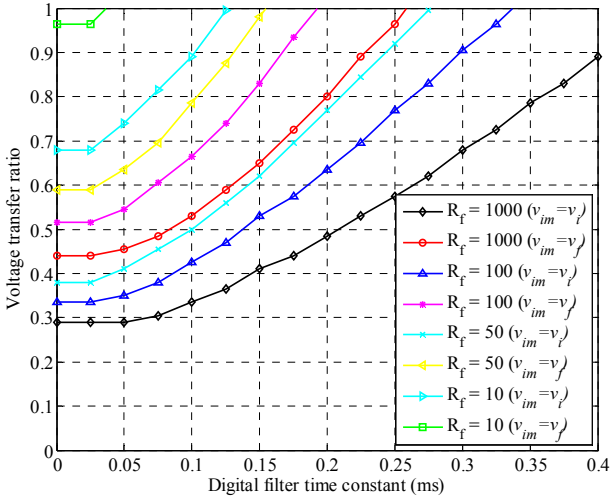

Fig. 6 Effect of digital voltage measurement point, input filter resistance and digital filter time constant (RLC filter case) on stability.

By using the v_f as input to the modulation algorithm, the stable operating region is increased as does the previous case. Lower values of the input filter resistance will extend the stable operating region. However, the resistance will increase the filter losses. In addition, this voltage measurement strategy may deteriorate the input power factor [2]. In the following section, the significant change of losses and power factor are evaluated.

4   Effects of Input Filter
4.1   Loss

The input filter resistance increases the stability of the MC drive system as shown in the previous section. The scope of this section is to calculate the steady state

losses resulting from the filter resistance. Referring to Fig. 3(b) we have:

$$\bar{I}_r = \frac{j\omega_i L_f}{R_f + j\omega_i L_f} \bar{I}_s \tag{33}$$

where $\bar{I}_r$ is the input filter resistance current. The capital letters are used to define variables in steady state condition. Therefore, the power loss in the input filter is:

$$P_{loss} = R_f \mid \frac{j\omega_i L_f}{R_f + j\omega_i L_f} \bar{I}_s \mid^2 \tag{34}$$

With definition of output power as:

$$P_{out} = R_o \mid \frac{q\bar{V}_i}{Z_o} \mid^2 \tag{35}$$

the matrix converter efficiency can be calculated. Fig. 7 shows that the efficiency of the system is almost 100 % even for the smallest value of the filter resistance. Therefore, choosing a suitable value for the filter resistance to ensure the stability does not decline the efficiency.

4.2   Phase Shift

If the parallel combination of an inductor and a resistor of the RLC input filter causes a large phase difference between $\bar{v}_i$ and $\bar{v}_f$, the input power factor will no longer be unity when the voltage is measured across the filter capacitor. To determine the phase shift, the voltage drop across the filter can be calculated by:

$$\bar{V}_{drop} = \frac{j\omega_i L_f R_f}{R_f + j\omega_i L_f} \bar{I}_s \tag{36}$$

Substituting $\bar{I}_s$ from Eq. (15) in Eq. (36) leads to:

$$\bar{V}_{drop} = \frac{j\omega_i L_f R_f}{R_f + j\omega_i L_f} (j\omega_i C_f + \frac{R_o}{Z_o^2} q^2)\bar{V}_i \tag{37}$$

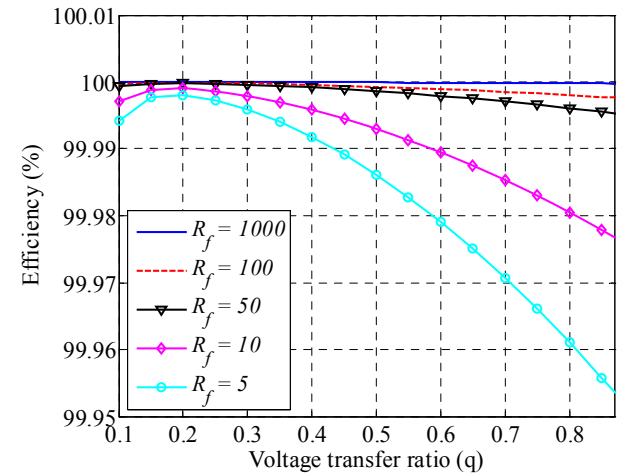Regarding $R_f \gg \omega_i L_f$ the above expression is simplified as:

Fig. 7 Effect of the input filter resistor and the voltage transfer ratio on the MC loss.

$$\overline{V}_{drop} = \frac{\omega_i R_o}{L_f Z_o} q^2 \mid \overline{V}_i \mid \angle(\frac{\pi}{2} - \tan^{-1}(PF_{load})) \qquad (38)$$

where PFload is the load power factor. For parameters shown in Table 1, we have $\omega_i R_o L_f / Z_o^2 = 0.017$ which yields $\mid \overline{V}_{drop} \mid \le 0.01 \mid \overline{V}_i \mid$. Therefore, the voltage drop across the input filter is negligible, so a considerable phase shift is not introduced between $\overline{v}_i$ and $\overline{v}_f$.

4.3 Frequency Response

The LC filter input current transfer function in Laplace (s) space is

$$I_s(s) = \frac{C_f s}{1 + L_f C_f s^2} V_f(s) + \frac{1}{1 + L_f C_f s^2} I_i(s) \qquad (39)$$

and for the RLC filter we have

$$I_s(s) = \frac{(R_f + L_f s) C_f s}{R_f + L_f s + L_f C_f s^2} V_f(s) + \dots$$
$$\frac{R_f + L_f s}{R_f + L_f s + L_f C_f s^2} I_i(s) \qquad (40)$$

Therefore, the grid current (I_s) is affected by input voltage (V_f) and the MC input current (I_i). The filter should eliminate the switching harmonics of I_i to increase the quality of the grid current. Fig. 8 shows the frequency response of the transfer function between the input and the grid currents. There is the possibility of magnification of the input current distortions at the filter resonance frequency. The resonance frequency is calculated by $f_{res} = 1 / 2\pi\sqrt{L_f C_f}$.

However, the resonance can be avoided by a proper choice of filter resistance. Fig. 8 shows that for $R_f = 5$ Ω, the magnitude of the frequency response is greatly reduced. Therefore, the input current distortions are not amplified. Lower values of filter resistance decrease the magnitude of the resonance but at the same time will lower the filter ability in alleviating the input filter distortions. Fig. 9 shows the effect of the filter resistance on the frequency response magnitude at the switching frequency. By reducing the Rf values the filter ability in switching harmonic elimination is decreased. As a result, the values of filter resistance should be chosen as a compromise between the harmonic reduction and the distortion amplification resulting from resonance.

It can be concluded that by using an RLC filter, measuring the voltage at filter input and a proper choice of filter resistance, the stable operation is provided and the need for the digital filter is eliminated.

5 Simulation Results

The benchmark system shown in Fig. 2 is simulated using PSCA/EMTDC software to confirm the results of the proposed analysis. The Space Vector Modulation (SVM) algorithm is implemented.
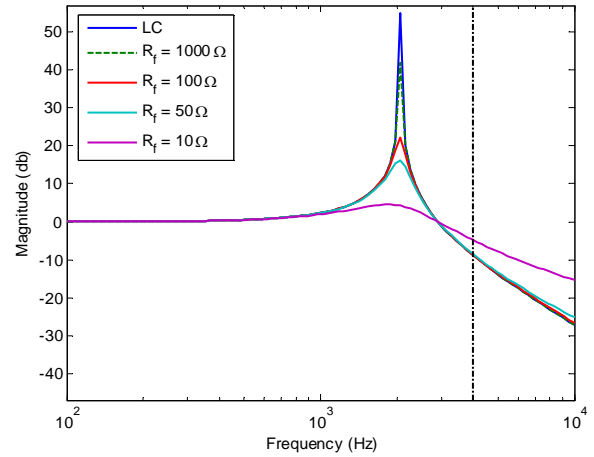

Fig. 8 The frequency response of LC and RLC input filters.
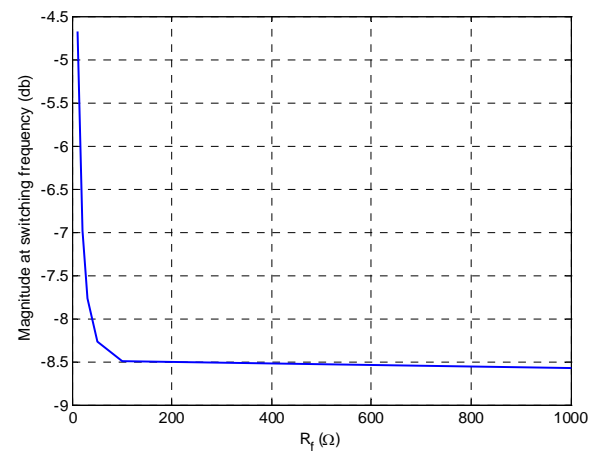

Fig. 9 Magnitude of RLC filter frequency response at switching frequency.

Fig. 10(a) shows when the digital filter time constant is zero, in case of the LC filter and the measured voltage at the terminal of the filter capacitor, the system will move towards the unstable region if q is greater than 0.33. From the results presented in Fig. 4, clearly without using the digital filter, the MC is unstable when q is beyond 0.3. Therefore, the simulation and analytical results are in good agreement. As it is clear from Fig. 4, for the stable operation of the MC the digital filter time constant should be around 0.4 msec. This result is approved by simulation as shown in Fig. 10(b). For $\tau = 0.4$ msec, the MC system is stable for q between 0.1 and 0.87. The digital filter reduces the input voltage distortion passes through modulation algorithm. When the filter time constant is too low, its speed increases and the distortion may affect the calculation of input voltage angle. On the other hand when the time constant is too high, the filter dynamic reduces the speed of the system, so the input voltage distortions will appear at the output side. Therefore, a tradeoff should be made between the speed and stability of the system. By value of $\tau = 0.4$ ms both speed and stability are guaranteed for $0 < q < 0.87$.
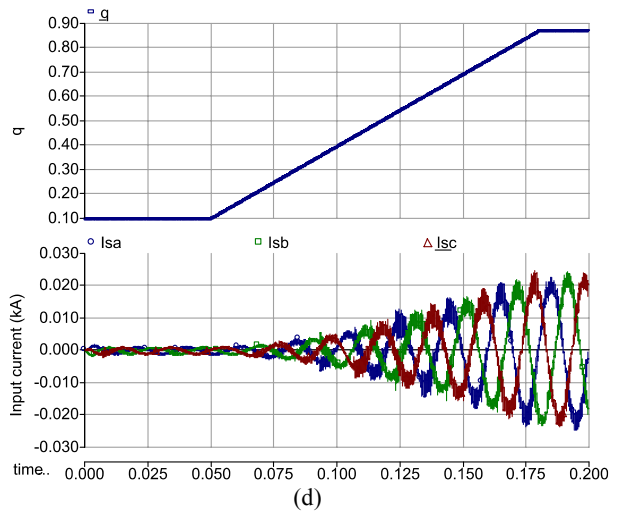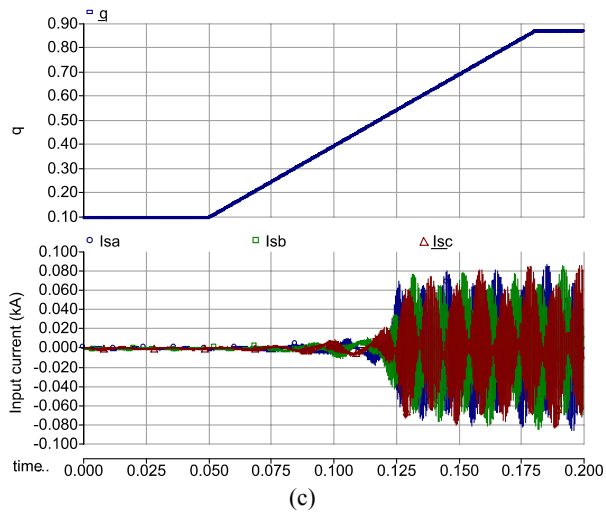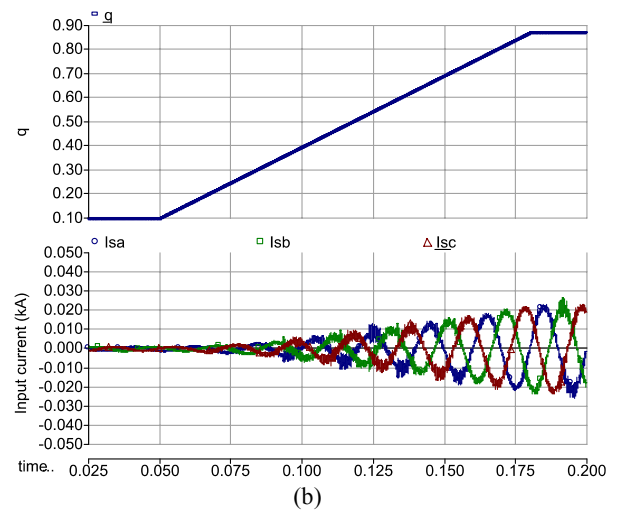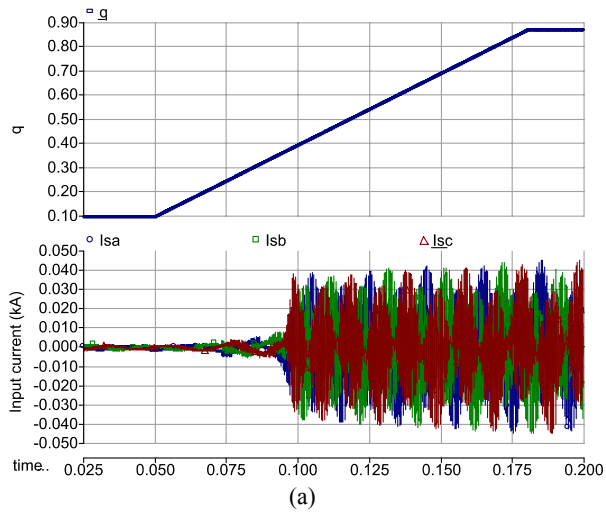
Fig. 10 The voltage transfer ratio (upper) and the input current (bottom) of the matrix converter for the LC input filter configuration (a) $\tau=0, \bar{y}_{im} = \bar{v}_i$, (b) $\tau=0.4\,\text{ms}, \bar{y}_{im} = \bar{v}_i$, (c) $\tau=0, \bar{y}_{im} = \bar{v}_f$, (d) $\tau=0.4\,\text{ms}, \bar{y}_{im} = \bar{v}_f$.
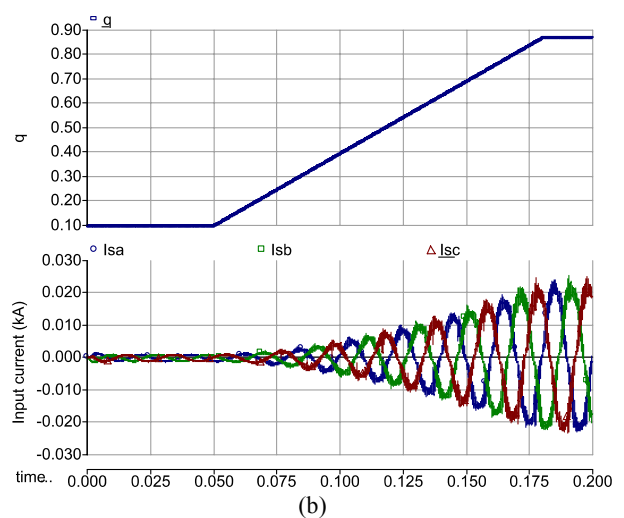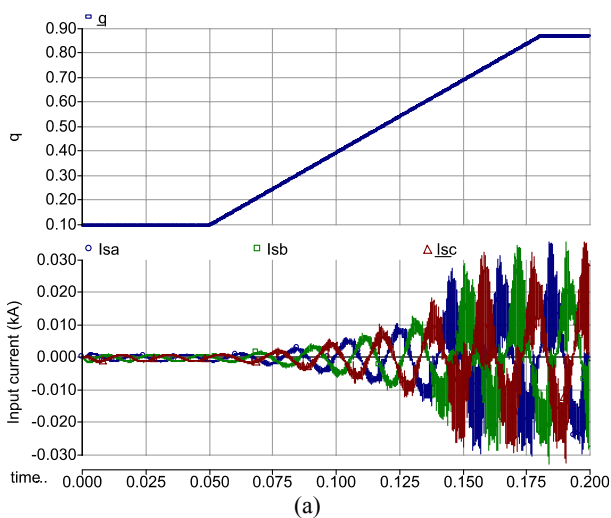

Fig. 11 The voltage transfer ratio (upper) and the input current (bottom) of the matrix converter for the RLC input filter configuration (a) $\tau=0, \bar{y}_{im} = \bar{v}_i$ (b) $\tau=0, \bar{y}_{im} = \bar{v}_f$.
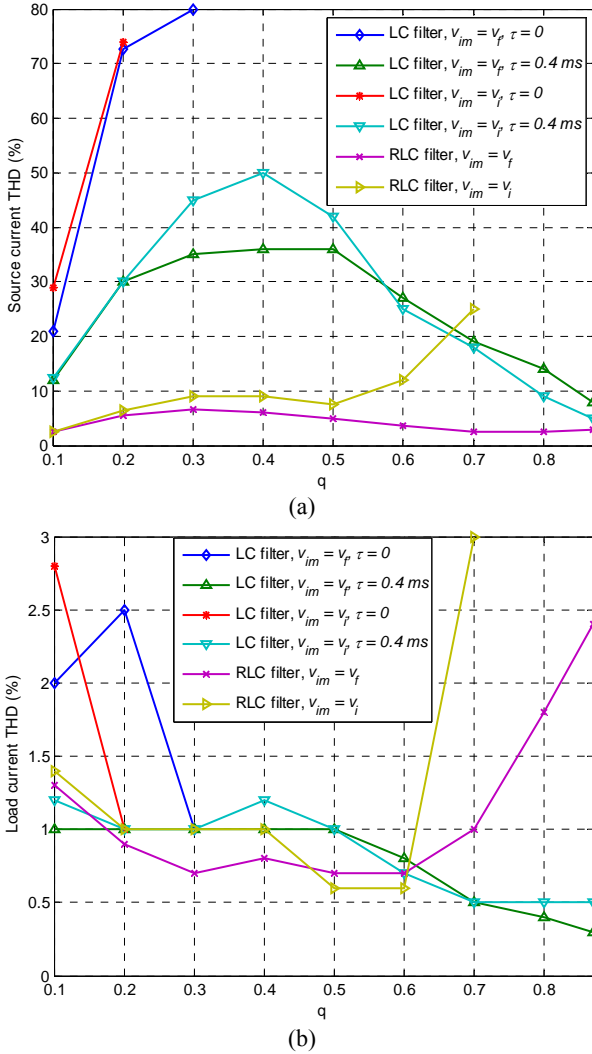
Fig. 12 THD of (a) source current, and (b) load current for different input filters and digital filter time constant.

If the voltage measurement point is at the input filter ($v_{im} = v_f$), in the absence of the digital filter, the analytical result shown in Fig. 10(c) reveals that when q is greater than 0.47 the system is unstable. The simulation result shows that for stable operation the maximum limit of q to be 0.43. Therefore, the simulation results validate the findings of the linear system eigenvalue analysis in this case.

This system can be stabilized by an appropriate choice for τ which can be any value greater than 0.25 ms according to Fig. 4. By supposing $\tau = 0.25$ ms, the simulated three phase input currents shown in Fig. 10(d) are stable independent of the value of q. It can be concluded that the eigenvalue analysis can be a proper tool to evaluate the stability if the LC input filter is used.

Fig. 11(a) shows that without using the digital input filter, even if the voltage is measured at the filter input and the RLC filter is used, the system experiences instability for q greater than 0.61. The filter resistance is

10 Ω. Fig. 6 demonstrates that for this value of filter resistance, the maximum limit of *q* prior to instability is 0.68. The analytical and simulation results render a good agreement. For this configuration and the given set of parameters, using $\bar{v}_f$ for the modulation algorithm ensures stable operation over all q values as shown in Figs. 6 & 11(b). In this case, there is no need for a digital filter.

Fig. 12 shows the THD of the source and load currents for the LC and the RLC filter types. For the LC filter type, the THD is plotted with and without a digital filter.

Regarding the source current, Fig. 12(a) indicates that using the RLC filter type and measuring the modulation voltage at point before the input filter leads to a minimum current distortion with a maximum THD value below 7%. Without using the digital filter, the source current of the system with the LC filter is distorted. The digital filter can stabilize this system; however, the THD of the source current remains considerably higher than the acceptable range.

The THD of load current shown in Fig. 12(b) indicates that the load current contains negligible distortions for all cases as long as the system is stable. This is an interesting characteristic of the matrix converter as generates the high-quality output current even if the input current is highly distorted. Moreover, in the presence of a digital filter besides the advantage of increased the stable operating range, the load current quality will be improved when the LC filter configuration is used.

6   Conclusion

With respect to stability issue, the performed analytical and simulation studies have shown that the RLC input filter configuration provides a superior operation of MC,s over the LC filter. Moreover, when the modulation algorithm is fed by the voltage derived at the input filter will further improve the stability of the system. A proper choice of the filter resistance along with the use of the measured voltage at the input filter leads to stable operation of the system over all the voltage ratio ranges: (0 < q < 0.87). This simplifies the modulation algorithm in the absence of the digital filter at the input voltage. However, the power loss and the drop of efficiency corresponding to filter resistance and also the deviation of the input power factor from unity can be the drawbacks. These are calculated and shown that the drop of efficiency arising from the filter resistance is below 0.1 %, and as the voltage drop across the input filter resistance is quite small compared to the input voltage, the change in the input power factor is negligible.

Appendix

$$\mathbf{A}_{11} = \begin{bmatrix} -R_s/L_t & \omega_i & -1/L_t & 0 \\ -\omega_i & -R_s/L_t & 0 & -1/L_t \\ 1/C_f & 0 & 0 & \omega_i \\ 0 & 1/C_f & -\omega_i & 0 \\ 0 & 0 & q/L_o & 0 \\ 0 & 0 & 0 & 0 \\ 0 & 0 & -1/\tau & 0 \\ 0 & 0 & 0 & 1/\tau \end{bmatrix} \tag{A-1}$$

$$\mathbf{A}_{12} = \begin{bmatrix} 0 & 0 & 0 & 0 \\ 0 & 0 & 0 & 0 \\ -q/C_f & 0 & q^2 R_o/C_f Z_o^2 & 0 \\ 0 & 0 & 0 & -q^2 R_o/C_f Z_o^2 \\ -R_o/L_o & \omega_o & -q/L_o & 0 \\ -\omega_o & -R_o/L_o & 0 & 0 \\ 0 & 0 & -1/\tau & 0 \\ 0 & 0 & 0 & -1/\tau \end{bmatrix} \tag{A-2}$$

$$\mathbf{A}_{21} = \begin{bmatrix} \dfrac{-R_s}{L_t} & \omega_i & \dfrac{-1}{L_t} & 0 \\[6pt] -\omega_i & \dfrac{-R_s}{L_t} & 0 & \dfrac{-1}{L_t} \\[6pt] \dfrac{1}{C_f} & 0 & 0 & \omega_i \\[6pt] 0 & \dfrac{1}{C_f} & -\omega_i & 0 \\[6pt] 0 & 0 & \dfrac{q}{L_o} & 0 \\[6pt] 0 & 0 & 0 & 0 \\[6pt] \dfrac{-R_s L_f}{\tau L_t} & 0 & \dfrac{-1}{\tau} & 0 \\[6pt] 0 & \dfrac{-R_s L_f}{\tau L_t} & 0 & \dfrac{L_s}{\tau L_t} \end{bmatrix} \tag{A-3}$$

$$\mathbf{A}_{22} = \mathbf{A}_{12} \tag{A-4}$$

$$\mathbf{A}_{31} = \begin{bmatrix} \dfrac{-(R_s+R_f)}{L_s} & \omega_i & \dfrac{R_f}{L_s} & 0 & -1/L_s \\[6pt] -\omega_i & \dfrac{-(R_s+R_f)}{L_s} & \dfrac{R_f}{L_s} & 0 & 0 \\[6pt] R_f/L_f & 0 & \dfrac{-R_f}{L_f} & \omega_i & 0 \\[6pt] 0 & R_f/L_f & -\omega_i & \dfrac{-R_f}{L_f} & 0 \\[6pt] 1/C_f & 1/C_f & 0 & 0 & 0 \\[6pt] 0 & 0 & 1/C_f & 0 & -\omega_i \\[6pt] 0 & 0 & 0 & 0 & q/L_o \\[6pt] 0 & 0 & 0 & 0 & 0 \\[6pt] 0 & 0 & 0 & 0 & 1/\tau \\[6pt] 0 & 0 & 0 & 0 & 0 \end{bmatrix} \tag{A-5}$$

$$\mathbf{A}_{32} = \begin{bmatrix} 0 & 0 & 0 & 0 & 0 \\ -1/L_s & 0 & 0 & 0 & 0 \\ 0 & 0 & 0 & 0 & 0 \\ 0 & 0 & 0 & 0 & 0 \\ \omega_i & -q/C_f & 0 & \gamma & 0 \\ 0 & 0 & 0 & 0 & \gamma \\ 0 & -R_o/L_o & \omega_o & -q/L_o & 0 \\ 0 & -\omega_o & R_o/L_o & 0 & 0 \\ 0 & 0 & 0 & -1/\tau & 0 \\ 1/\tau & 0 & 0 & 0 & -1/\tau \end{bmatrix} \tag{A-6}$$

where $\gamma = q^2 R_o/C_f Z_o^2$.

$$\mathbf{A}_{41} = \begin{bmatrix} -(R_s+R_f)/L_s & \omega_i & R_f/L_s & 0 & -1/L_s \\ -\omega_i & 0 & 0 & R_f/L_s & 0 \\ R_f/L_f & 0 & -R_f/L_f & \omega_i & 0 \\ 0 & 0 & -\omega_i & -R_f/L_f & 0 \\ 1/C_f & 0 & 0 & 0 & 0 \\ 0 & 0 & 1/C_f & 0 & -\omega_i \\ 0 & 0 & 0 & 0 & q/L_o \\ 0 & 0 & 0 & 0 & 0 \\ R_f/\tau & 0 & -R_f/\tau & 0 & 1/\tau \\ 0 & R_f/\tau & 0 & -R_f/\tau & 0 \end{bmatrix} \tag{A-7}$$

$$\mathbf{A}_{42} = \begin{bmatrix} 0 & 0 & 0 & 0 & 0 \\ -1/L_s & 0 & 0 & 0 & 0 \\ 0 & 0 & 0 & 0 & 0 \\ 0 & 0 & 0 & 0 & 0 \\ \omega_i & -q/C_f & 0 & \gamma & 0 \\ 0 & 0 & 0 & 0 & \gamma \\ 0 & -R_o/L_o & \omega_o & -q/L_o & 0 \\ 0 & -\omega_o & R_o/L_o & 0 & 0 \\ 0 & 0 & 0 & -1/\tau & 0 \\ 1/\tau & 0 & 0 & 0 & -1/\tau \end{bmatrix} \tag{A-8}$$

References

[1] P. W. Wheeler, J. Rodriguez, J. C. Clare, L. Empringham and A. Weinstein, "Matrix converters: a technology review". *IEEE Transactions Industrial Electronics*, Vol. 49, No. 2, pp. 276-288, April 2002.

[2] S. Kwak, "Indirect matrix converter drives for unity displacement factor and minimum switching losses", *Electeric Power System Research*, Vol. 77, No. 5, pp. 447-454, 2007.

[3] E. Ibarra, J. Andreu, I. Kortabarria, E. Ormaetxea, I. M. de Alegria, J. L. Martin and P. Ibanez, "New fault tolerant matrix converter", *Electeric Power System Research*, Vol. 81, No. 2, pp. 538-552, 2011.

[4] E. Ormaetxea, J. Andreu, I. Korabarria, U. Bidarte, I. M. de Alegria, E. Ibarra and E. Olaguuenaga, "Matrix converter protection and

computational capabilities based on a system on chip design with FPGA", *IEEE Transactions Power Electronics*, Vol. 26, No. 1, pp. 272–286, January 2011.

[5] A. Khajeh and R. Ghazi, "GA-Based Optimal LQR Controller to Improve LVRT Capability of DFIG Wind Turbines", *Iranian Journal of Electrical & Electronic Engineering*, Vol. 9, No. 3, pp. 167-176, 2013.

[6] D. Casadei, G. Serra, A. Tani and L. Zarri, "Stability analysis of electrical drives fed by matrix converter", in *IEEE International Symposium on Industrial Electronics*, pp. 1108-1113, 2002.

[7] F. Liu, C. Klumpner and F. Blaabjerg, "Stability analysis and expreimental evaluation of a matrix converter drive system", in *Annual Conference of the IEEE Industrial Electronics Society*, pp. 2059–2065, 2003.

[8] F. Liu, C. Klumpner and F. Blaabjerg ,"A robust method to improve stability in matrix converters", in *IEEE Power Electronics Specialists Conference*, pp. 3560-3566, 2004.

[9] E. Edrem, Y. Tatar and S. Sunter, "Effects of input filter on stability of matrix converter using venturini modulation algorithm", *International Symposium on Power Electronics, Electrical Drives, Automation and Motion*, pp. 1344-1349, 2010.

[10] D. Casadei, G. Serra, A. Tani and L. Zarri, "Effects of input voltage measurement on stabilityof matrix converter drive system", *IEE Proceeding on Electrical Power Applications*, Vol. 151, No. 4, pp. 487-497, 2004.

[11] D. Casadei, J. Clare, L. Empringham, G. Serra, A. Tani, A. Trentin and P. W. L. Zarri, "Large-signal model for the stability analysis of matrix converters", *IEEE Transactions Industrial Electronics*, Vol. 54, No. 2, pp. 939-950, 2007.

[12] S. M. Cox and P. Zanchetta, "Matrix converter systmes stability analysis taking into account switching effects", *European Conf. on Power Electronics and Applications*, pp. 1-10, 2011.

[13] S. M. Cox and J. C. Clare, "Nonlinear development of matrix-converter unstabilities", *Journal of Engineering Mathematics*, Vol. 67, No. 3, pp. 241-259, 2009.

[14] C. A. J. Ruse, J. C. Clare and C. Klumpner, "Numerical approach for guaranteeing stable design of practical matrix converter drive system", *Annual Conference on IEEE Industrial Electronics*, pp. 2630-2635, 2006.

[15] D. Casadei, G. Serra, A. Tani, A. Trentin and L. Zarri, "Theorical and exprimental investigation on the stability of matrix converters". *IEEE Transactions Industrial Electronics*, Vol. 25, No. 2, pp.1409-1419, October 2005.

[16] C. Xia, P. Song, T. Shi and Y. Yan, "Chaotic dynamics characteristic analysis for matrix converter", *IEEE Transactions Industrial Electronics*, Vol. 60, No. 1, pp. 78-87, 2013.

[17] D. Casadei, G. Serra, A. Tani and L. Zarri, "Matrix converter modulation strategies: a new general approach based on space-vector representation of the switch state", *IEEE Transactions Industrial Electronics*, Vol. 49, No. 2, pp. 370-381, 2002.

Mohamad Hosseini Abardeh received the B.Sc. degree in control engineering from Ferdowsi university of Mashhad in 2005, and the M.Sc. degree in power engineering from Tarbiat Modares University of Tehran, Iran in 2008. He is currently with electrical department of Azad University of Shahrood. His research interests are power electronic, power quality and renewable energies.

Reza Ghazi (M'90) was born in Semnan, Iran in 1952. He received his B.Sc., degree (with honors) from Tehran University of Science and Technology, Tehran, Iran in 1976. In 1986 he received his M.Sc. degree from Manchester University, Institute of Science and Technology (UMIST) and the Ph.D. degree in 1989 from University of Salford UK, all in electrical engineering. Following receipt of the Ph.D. degree, he joined the faculty of engineering Ferdowsi University of Mashhad, Iran as an Assistant Professor of electrical engineering. He is currently Professor of Electrical Engineering in Ferdowsi University of Mashhad, Iran. His main research interests are reactive power control, FACTS devices, application of power electronic in power systems, distributed generation, restructured power systems control and analysis. He has published over 100 papers in these fields including three books.